



ISSN: 0067-2904

Measurements of Linear and Nonlinear Optical Properties for Iraqi Heavy Crude Oil Samples

Hayder A. Naser^{*1}, Aseel I. Mahmood², Sawsan K. Fandi²

¹Imam Al-Kadhum College, Departments of Computer Techniques Engineering, Baghdad, Iraq

²Materials Research Directorate, Ministry of Science and Technology, Baghdad, Iraq

Received: 25/11/2020

Accepted: 7/6/2020

Abstract

In this work, linear and nonlinear optical properties of two types of Iraqi heavy crude oil extracted from fields in southern Iraq were determined. The nonlinear optical properties were measured utilizing Z-scan technology with He-Ne laser at 632.8 nm. It was found that nonlinear refractive index (NLR) values for the Basra and Kut heavy crude oil samples are 6.34381×10^{-4} and $8.25108 \times 10^{-4} \text{ cm}^2/\text{mW}$, respectively, while those for the nonlinear absorption coefficient (NLA) are $2.68942 \times 10^{-5} \frac{\text{cm}}{\text{mW}}$ and $2.58874 \times 10^{-5} \frac{\text{cm}}{\text{mW}}$, respectively. These results showed that the two samples with linear and nonlinear optical properties can be used in optics field applications as optical limiter devices at a wavelength of 632.8 nm.

Keywords: heavy crude oil, nonlinear refractive index, nonlinear absorption

قياس الخواص الضوئية الخطية واللاخطية لعينات من النفط الخام العراقي الثقيل

حيدر عايد ناصر^{1*}، اسيل إبراهيم محمود²، سوسن خلف فندي²

¹كلية الامام الكاظم، قسم هندسة تقنيات الحاسوب، بغداد، العراق

²دائرة بحوث المواد، وزارة العلوم والتكنولوجيا، بغداد، العراق

الخلاصة

في هذا العمل، تم تحديد الخواص البصرية الخطية وغير الخطية لاثنتين من الزيوت الخام العراقية الثقيلة المستخرجة من الحقول في جنوب العراق. تم قياس الخواص البصرية اللاخطية باستخدام تقنية المسح الضوئي باستخدام ليزر He-Ne عند 632.8 نانومتر. تبين أن معامل الانكسار اللاخطي (NLR) لعينات الزيت الخام في البصرة والكوت يبلغ 6.34381×10^{-4} و $8.25108 \times 10^{-4} \frac{\text{cm}^2}{\text{mW}}$ على التوالي، ومعامل الامتصاص اللاخطي (NLA) لكل منهما: $2.68942 \times 10^{-5} \frac{\text{cm}}{\text{mW}}$ و $2.58874 \times 10^{-5} \frac{\text{cm}}{\text{mW}}$ على التوالي. أظهرت هذه النتائج أنه يمكن استخدام العينات ذات الخصائص البصرية الخطية وغير الخطية في تطبيقات مجال البصريات كالمحددات البصرية عند الطول الموجي 632.8nm.

Introduction

Crude oil is simply a black liquid with a high viscosity that is extracted from the ground by special exploration operations. It is a mixture of a large amount of hydrocarbons, varying amount of waxes, and low content of asphalt [1]. The American Petroleum Institute (API) gravity is a measure of how heavy or light a petroleum liquid is compared to water; if API gravity is greater than 10, it is lighter and floats on water; if less than 10, it is heavier and sinks [2]. The heavy crude oil of Basra has an API value of 24° according to the Exxon Mobil index table. It is described to have high values of precise

*Email: hayder.a.naser@gmail.com

enormity, viscidness, contents of asphalt, and weight of hydrocarbons [3, 4]. It is usually extremely sticky, with a constancy ranging from that of weighty syrup to a solid at room temperature [5]. Oil studies are important strategic tools because of the importance of crude oil at different levels of strategic planning. Most of the previous specialized studies in this field have focused on improving the quality, thermal properties, extraction methods [6], linear optical properties [7], physical properties [8], and physico-chemical properties [9]. The refractive index of crude oil is related to the characteristics of the sample [10, 11]. Measuring of refractive index is difficult because of the high density of crude oil [12]. It is useful in studying various oil properties such as density and heat capacity [13]. This work examines the linear and non-linear optical properties of two heavy crude oil samples extracted from the Basra and Kut fields in southern Iraq by Z-scan technique to study these characteristics in suitable applications.

Dynamical model

The Z-Scan technique is a method often used to conclude the nonlinear possessions on definite materials [14, 15]. It is based on the principle of spatial distortion that a beam undergoes when passing through a material with properties of nonlinear optics [16]. It allows estimating the magnitude and the sign of the NLR through a sample [17]. As the sample moves in the direction of propagation, it undergoes a small change in the intensity that affects about the sample, which is due to the lens. Part of the radiation received by the sample is transmitted, which reaches an iris that will only pass a fraction of the transmitted radiation to be collected by the photo-detector. The signal that approaches the photo-detector is graded depending on the position of the sample with respect to the focus of the lens. The implementation of the Z-Scan technique was divided into different stages, namely open aperture (OA) and closed aperture (CA) [18]. The beam has the largest density in the center, so it will generate a change in the refractive index which forms a lens in the sample. The sample thickness (L) must be less than Rayleigh's length z_0 [19,20]. This permits to consider the interaction between the laser beam and the sample to happen at only one position and not to spread out over the entire interaction length [21]. The linear absorption coefficient (α_0) for a thin film sample was calculated by [22, 23]:

$$\alpha_0 = \frac{1}{L} \ln \frac{1}{T} \quad (1)$$

where L is the thickness of the sample and T is the transmittance. The reflectance (R) was calculated using the equation [24]:

$$\alpha_0 = \frac{1}{L} \ln \left(\frac{1-R}{T} \right) \quad (2)$$

In CA, when a laser beam is passed through the sample, its refractive index will change the output intensity. The phase shift ($\Delta\phi_0$) is determined by the change in output power intensity between peak and valley and is given by [25, 26].

$$\Delta T_{p-v} = 0.406(1-S)^{0.25} |\Delta\phi_0| \quad (3)$$

where ΔT_{p-v} is the difference between peak and valley of output power and S is the hole transmittance provided by [19], [27]:

$$S = \left(1 - \exp \left(-\frac{2r_a^2}{w_a^2} \right) \right) \quad (4)$$

where r_a is the hole radius and w_a is the beam radius at the hole. The sample is located at the center point of the lens, and then moved along the z axis at a coldness of $\mp z_0$, which is given by the Rayleigh length z_0 :

$$z_0 = \frac{\pi w_0^2}{\lambda} \quad (5)$$

where w_0 is the beam waist. The NLR is given by:

$$NLR = \frac{\Delta\phi_0}{k I_0 L_{eff}} \quad (6)$$

where k is the wave number, λ is the wavelength of the beam, I_0 is the laser intensity at focus, and L_{eff} is the effective length of the sample given by:

$$L_{eff} = (1 - \exp(-\alpha_0 L)) / \alpha_0 \quad (7)$$

where L is the sample thickness. When the iris is removed, in OA Z- scan, the detector collects the entire beam and causes this change in intensity to absorb the photon in the sample. The highest NLA is observed in very weak beam intensity due to nonlinear effects. The NLA is given by [27-28]:

$$NLA = \frac{2\sqrt{2} \Delta T}{I_0 L_{eff}} \quad (8)$$

where ΔT is the peak of the curve. The nonlinear optical efficiency/transparency which compromise (NLR / α_0) at a definite wavelength is therefore of main prominence for evaluating the appropriateness of a material for all-optical devices. This factor is typically estimated through two statistics of merit [29-31]:

$$W = \frac{(NLR)I}{\alpha_0 \lambda} \quad (9)$$

$$T = \frac{(NLA) \lambda}{NLR} \quad (10)$$

According to the previous requirements, it is essential to achieve $W \gg 1$ and $T \ll 1$.

Experimental Setup

In this work, a sample of the material under investigation is moved through the focus of a laser beam, and the beam radius (or the on-axis intensity) is measured at some point behind the focus as a function of the sample position (Figure-1). A computerized stepper motor was used to move the sample along the z- axis with a steep of 10 μm . An Arduino board was programmed to read the output intensity from a light source directly and from the moving sample by using two silicon detectors. Then, these outputs were programmed and simulated. A He-Ne laser with a wavelength of 632.8nm and an output power of 5mW was focused to a small spot by a positive lens with a focal length of 15 cm. The focused beam was passed through the two crude oil samples with 2 mm thickness of each sample. Figure-1 shows the experimental setup of the submitted system. A TEM00 Gaussian beam has the highest intensity at the center and will produce a change in the index of refraction, creating a lens in the tested sample. The measured laser intensity (I_0) is 67634.71 mW cm^{-2} and the radius of the beam at the iris (w_0) is 15114.6496 nm.

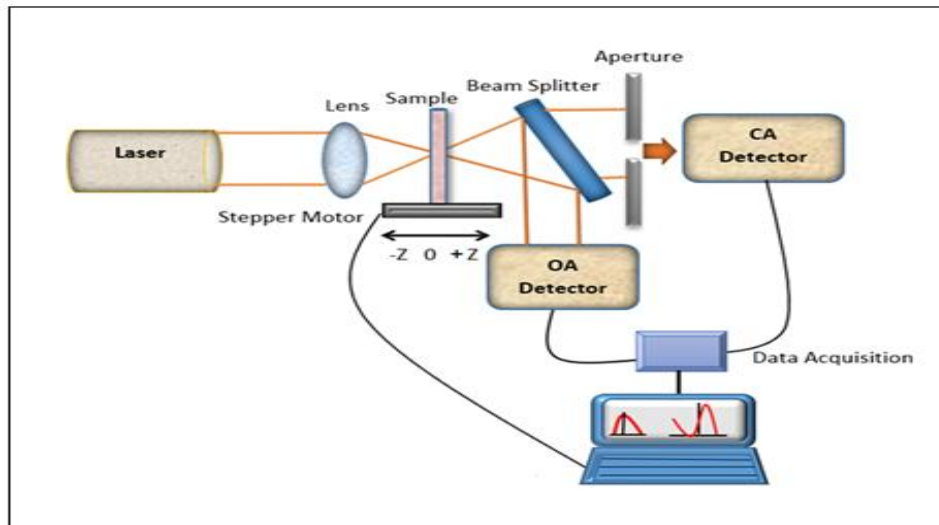


Figure 1-Description of the experimental setup.

The beam waist (w_0) at the focal point is 2.4183×10^4 nm while the Rayleigh length (z_0) is 29 mm and the hole transmittance (S) is 2.188638×10^{-9} . The effective length (L_{eff}) values are 1.438 and 1.5039612 for the Basra and Kut heavy crude samples, respectively. The CA and OA were achieved, respectively, with an iris of 1 mm.

Results and Discussion

The absorbance spectra for the two samples are shown in Figure-2.

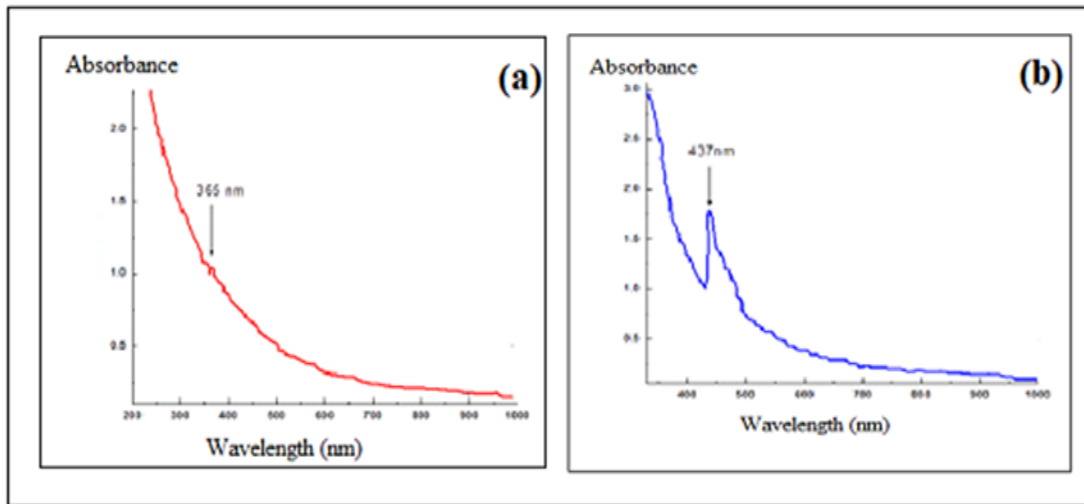


Figure 2-The spectral behavior of the two heavy crude oil samples: (a) Basra sample , (b) Kut sample. The peaks on this curve represent the suitable wavelength for these samples to find their nonlinear properties.

The achieved consequences of the linear properties of the two samples are shown in Table-1.

Table 1-The optical parameters and the calculated linear absorption coefficient

Material	Linear absorption coefficient α_0 (mm) ⁻¹	Reflectance (R)	Thickness of model d (mm)	Wavelength λ (nm)
Basra sample	0.35	2.351	2	632.8
Kut sample	0.3	2.114	2	632.8

As the sample moves through the focused beam, self-focusing or defocusing adjusts the wave front phase, thus adapting the noticed beam intensity. Figure-3 explains the samples behavior for CA, which exhibits an NLR with a negative signal. At first, the beam of He-Ne laser shows a low NLR value at $Z < 0$. When the sample is becoming closer to the focus, the beam intensity is increasing, producing self-focusing, so a collimated beam is obtained at the iris. When the sample is enthused near the focus, this effect is decreased with increasing laser beam intensity due to the sample non linearity. The beam concentration is increasing again at $Z > 0$.

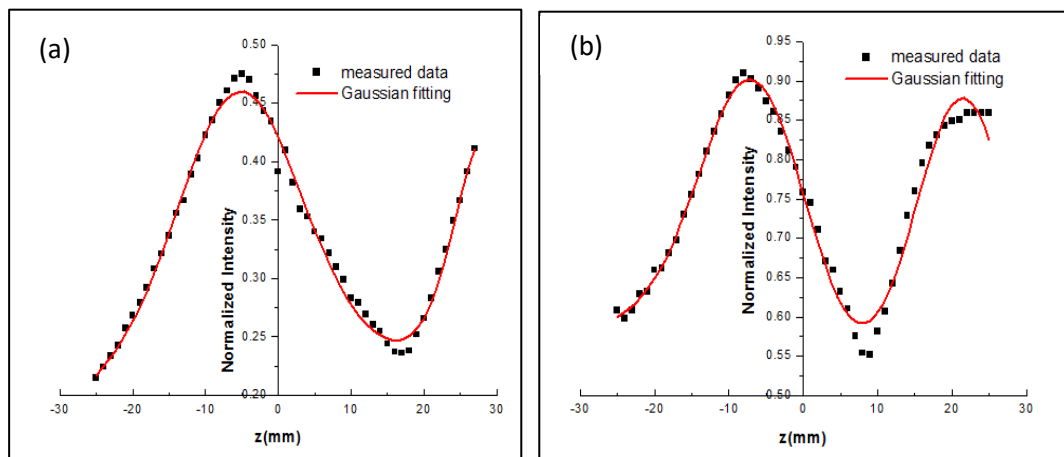


Figure 3-CA normalized transmittance curve :(a) Basra sample with $\Delta T_{p-v} = 0.238$, (b) Kut sample with $\Delta T_{p-v} = 0.358$.

The values of NLR obtained by CA from the two samples are listed in Table-2.

Table 2-The experimental results for the tested samples in CA

material	ΔT_{p-v}	$\Delta\phi_0$	$NLR(\frac{cm^2}{mW})$
Basra Sample	0.25	0.615897	6.34381×10^{-4}
Kut Sample	0.34	0.837620	8.25108×10^{-4}

In OA (Figure-4), the transmittance curve at $Z = 0$ is the minimum and the sample acts as a separating lens. The permeability is increasing linearly toward + Z axis at the furthest distance from the sample. This variation is due to the saturated absorption of the sample when the laser beam travels through the sample.

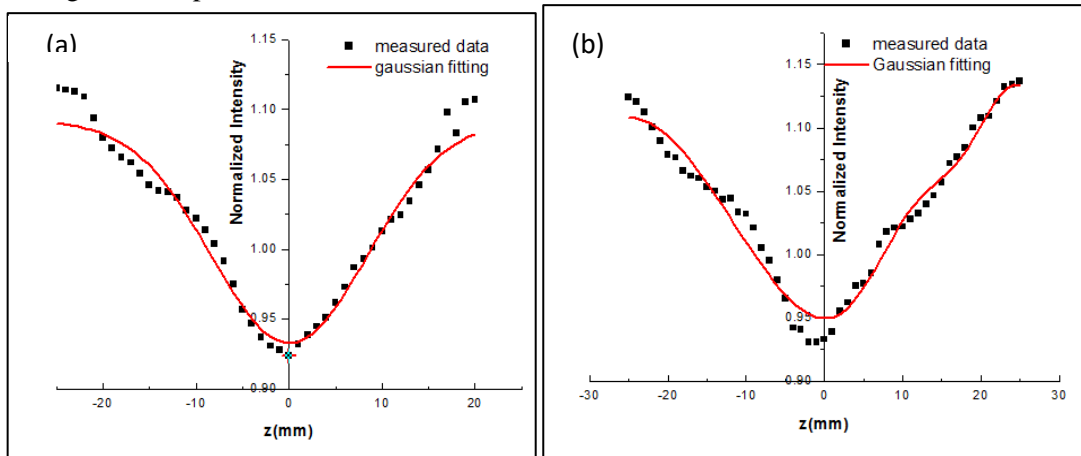


Figure 4-The OA Z- scan curve of experimental data: (a) for the Basra sample with $T=0.924$. (b) for the Kut sample with $T= 0.938$. Black circles represent the normalized intensity. The solid curves are the Gaussian fitting.

The values of NLA obtained by OA from the two samples are listed in Table-3.

Table 3-The experimental results for the two samples in OA

Material	T_{min}	$NLA(\frac{cm}{mW})$
Basra Sample	0.924	2.68942×10^{-5}
Kut Sample	0.938	2.58874×10^{-5}

In order to obtain more accurate results, the severity results in the case of CA are divided by the results of OA for the two samples (Figure-5).

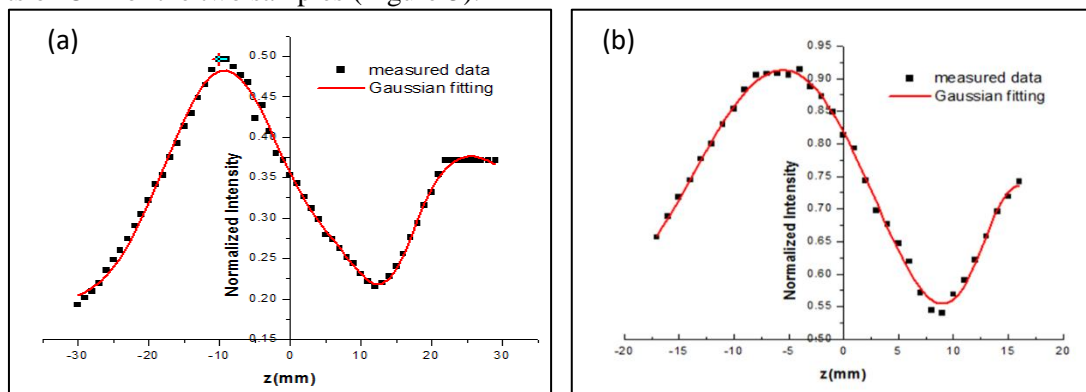


Figure 5-Z-scan experimental data by dividing CA/OA: (a) Basra sample, $\Delta T_{p-v} = 0.282$, (b) Kut Sample, $\Delta T_{p-v} = 0.374$.

Since the two samples exhibit relatively high linear absorption α_0 and NLA, The values of W and T, which are obtained by Eq. (9) and Eq. (10), did not satisfy the required conditions for the suitability of a material for all-optical integrated devices, i.e., $W \gg 1$ and $T \ll 1$. Hence, these samples are not

suitable to be used as optical switching devices. While some organo-metallic complexes satisfy these requirements [30].

Conclusions

The values of the linear absorption coefficient of Basra and Kut heavy crude samples are 0.35 and 0.3, respectively, while the reflectance values of these samples are 2.352 and 2.114, respectively. The optical results showed linear properties with high absorbance of UV radiation for the two samples. This might be dependent on the content of asphaltene and the high viscosity. The value of the NLR for the two samples are 6.34381×10^{-4} and $8.25108 \times 10^{-4} \frac{\text{cm}^2}{\text{mW}}$, while those of NLA are 2.68942×10^{-5} and $2.58874 \times 10^{-5} \frac{\text{cm}}{\text{mW}}$, respectively. The sign of NLR of the two samples was negative. Hence, they are considered as promising candidates to be used as optical limiting devices at the wavelength of 632.8 nm. The presence of a strong NLA produces good optical limiting. Both Basra and Kut samples unsatisfied the suitability to be used as optical switching at 632.8 nm.

References

1. Johnsen, E.E. and Ronningsen, H. P. **2003**. Viscosity of live water-in-crude-oil emulsions: experimental work and validation of correlations. *J. Pet. Sci. Eng.* **38**(12): 23–36.
2. Sanchez-Reyna, C. G., Ancheyta, G., Munoz, J. and Cardona, J. N. **2011**. Testing various mixing rules for calculation of viscosity of petroleum blends. *Fuel*, **90**: 3561–3570.
3. Castro, L.V. and Vazquez, F. **2009**. Fractionation and characterization of Mexican crude oils. *Energy Fuel*, **23**: 1603–1609.
4. Speight, J. G. **1991**. *The Chemistry and Technology of Petroleum*. Marcel Dekker, Inc.
5. Hasan, S. W., Ghannam, M. T., and Esmail, N. **2010**. Heavy crude oil viscosity reduction and rheology for pipeline transportation. *Fuel*, **89**: 1095–1100.
6. Santos, R. G., Loh, W., Bannwart, A. C., and Trevisan, O. V. **2014**. An Overview of Heavy Oil Properties and Its Recovery and Transportation Methods. *Brazilian Journal of Chemical Engineering*, **31**(03): 571 – 590.
7. Matoug, M. **2017**. Optical Techniques for Crude Oil and Asphaltene Characterization, MSc Thesis of applied science. University of Victoria.
8. Chuikina, D. I., Russkikh, I. V., Stakhina, L. D. and Serebrennikov, O. V. **2017**. Investigation of the Composition of High-Viscosity and Heavy Oils in the Course of EOR-Process Simulation, Journal of Siberian Federal University. *Chemistry*, **2**: 206-215.
9. Akbari, S., Abdurahman, N. H. and Fayaz, F. **2015**. The Influence of Process Parameters on Stability of Water –In crude Oil Emulsion Stabilized by Span 80. *international journal of engineering science & research technology*, **4**(5).
10. Riazi, M.R. and Roomi, Y.A. **2001**. Use of the refractive index in the estimation of thermophysical properties of hydrocarbons and petroleum mixtures. *Industrial & engineering chemistry research*. **40**(8): 1975-1984.
11. Yarranton, H.W., Okafor, J.C., Ortiz, D.P. and Van Den Berg, F.G.A. **2015**. Density and refractive index of petroleum, cuts, and mixtures. *Energy & Fuels*, **29**(9): 5723-5736.
12. Taylor, S.D., Czarnecki, J. and Masliyah, J. **2001**. Refractive index measurements of diluted bitumen solutions. *Fuel*, **80**(14): 2013-2018.
13. Mullins, O.C., Pomerantz, A.E., Zuo, J.Y. and Dong, C. **2014**. Downhole fluid analysis and asphaltene science for petroleum reservoir evaluation. *Annual review of chemical and biomolecular engineering*, **5**: 325-345.
14. Sheik-Bahae, M., Said A. A., Wel, T., Hagan, D. J. and Van Atryland, E. W. **1990**. Sensitive measurement of optical non-linearities using a single beam, *IEEE J. Quantum Electron.* **26**(4): 760-769.
15. Menard, J. **2007**. Single-beam differential z-scan technique, *Applied Optics*. **46**(11): 2119-2122.
16. Rekha, R. K. and Ramalingam, A. **2008**. Non-linear characterization and optical limiting effect of carmine dye, *Indian Journal of Science and Technology*. **2**(80).
17. Mendez, O. **2010**. Medicion del ndice de refraccion no-lineal positivosy negativos en muestras de colorantes en solucion, Junio.
18. Winter, C. S., Manning, R. J., Oliver, S. N. and Hill, C. A. **1992**. Optics Communications, **90**: 139-143.

19. Nader, R., Al-Hamdani A. H., Ibrahim, S. I. and Abd Ullah R. A. **2015**. Non-linear properties for Membranes of Rhodamine tincture by using Z-Scan Technique, *IJAIEEM*. **4**: 52-57.
20. Munnich, M. and Deflection, B. **2013**. MSc thesis, University of Central Florida.
21. Khurgin, J. B, Sun G. and Tsai D. P. **2015**. Ultrafast Thermal Nonlinearity, scientific reports: 1-8.
22. Yahya, N. Z. and Rusop, M. **2012**. Investigation on the Optical and Surface Morphology of Conjugated Polymer MEH-PPV:ZnO Nanocomposite Thin Films, *Journal of Nanomaterials*: 793679. 2012.
23. Abdullah, H., Selmani, S., Norazia, M. N., Menon, P. S., Shaari, S. and Dee, C. F. **2011**. ZnO:Sn Deposition by Sol-Gel Method: Effect of Annealing on the Structural, Morphology and Optical Properties, *Sains Malaysiana*. **40**(3): 245-250.
24. Hamdalla, T. A., Hanafy, T. A. and Bekheet, A. E. **2015**. Influence of Erbium Ions on the Optical and Structural Properties of Polyvinyl Alcohol, Hindawi Publishing Corporation. *Journal of Spectroscopy*.
25. Moran, M. J., She, C. Y. and Carman, R. L. **1975**. Interferometric Measurements of Nonlinear Refractive- Index Coefficient Relative to CS₂ in Laser- System- Related Materials, *IEEE J. Quantum Electron*. **11**: 259-263.
26. Owyong, A. **1973**. Ellipse Rotations Studies in Laser Host Materials, *IEEE J. Quantum Electron*. **9**: 1064 – 1069.
27. Stryland, E. W. **1998**. Z-Scan Measurements of Optical Nonlinearities, Characterization Techniques and Tabulations for Organic Nonlinear Materials”, *Florida*: 655-692.
28. Ule, E. **2015**. Measurement of The Nonlinear Refractive Index by Z-scan Technique, *Ljubljana*.
29. Fan, H. L., Ren, Q., Wang, X. Q., Li, T. B., Sun, J., Zhang, G. H., Xu, D., Yu, G. and Sun, G. H. **2009**. Investigation on Third-Order Optical Nonlinearities of Two Organometallic Dmit2-Complexes Using Z-Scan Technique, *Natural Science*. **1**(2): 136-141.
30. Sun, J. and Zhao, J. **2014**. Third-Order Nonlinear Optical Properties of an Organo-Metallic Complex, International Conference on Mechatronics, *Electronic, Industrial and Control Engineering*: 1303-1306.
31. Chena, Q. and Sargent, E. H. **2003**. Ultrafast Nonresonant Third-Order Optical Nonlinearity of a Conjugated 3, 38-Bipyridine Derivative from 1150 to 1600 nm, *Applied Physics Letters*. **82**(25): 4420-4422.